Applied Mathematics & Information Sciences
An International Journal

http://dx.doi.org/10.18576/amis/100613

A Study on the Behavior of Electromagnetic Waves for A Curved Antenna

*Elsayed Dahy**, *Afza Shafie and Noorhana Yahya*

Department of Fundamental and Applied Sciences, Universiti Teknologi PETRONAS, Seri Iskandar, 31750 Tronoh, Perak, Malaysia.

Received: 2 May 2016, Revised: 20 Jul. 2016, Accepted: 24 Jul. 2016
Published online: 1 Nov. 2016

Abstract: This paper discuss the potential of a curved electric dipole (of radius $R = r = h$) as a source of electromagnetic waves. We will present the solution of Maxwell equations in one dimension for the antenna. Green functions are employed to solve the toroidal and poloidal modes of the antenna, Simulations are carried out for a frequency range of 0.01 to 10Hz. Results have shown that the antenna is able to detect resistive layers under the sea bed.

Keywords: Electromagnetic wave, Maxwell equation, curve electric dipole

1 Introduction

To detect hydrocarbon beneath the sea bed there many techniques,one of them is the Control source electromagnetic (CSEM). This method employ made electric and magnetic field to excite the earth beneath the sea floor [9], [5], [12] and [16]. In this method, a horizontal electric dipole (HED) ([7]) is used to transmit ultra low frequency (0.1 - 5Hz) electromagnetic waves which is being located approximately 30 - 40m above the seabed to detect resistivity contrasts in the subsurface.

Control Source Electromagnetic (CSEM) theory makes use of the known theory of propagation within medium of varying resistivity contrast. An EM field is prompted into a conductive subsurface and propagated downwards and deep. Spatial distribution of resistivity from the many layers causes the wave behavior and characteristics to be slightly or majorly altered to depict the matter making the subsurface. Marine environment consists of or are made up of highly conductive sediments filled up with salt water. On the other hand some sediments are filled up with more resistive matter such as hydrocarbons and gases. Volcanic rocks and carbonates also represent some of resistive bodies that comprise the subsurface. Resistive constituents of the inhomogeneous subsurface reflect and propagates back to the seafloor some signal which is recorded by receivers equipped with electric and magnetic sensors.

Marine magnetotelluric MT method has been used in the study of the resistivity of seafloor. Among the studies are those conducted in [3], and [6]. They proposed the use of HED controlled-source sounding to study seafloor geology and expanded the concept of marine CSEM to describe a deep-sea experiment. Recent applications of magnetometric resistivity to the marine environment are given in [8], [18], [4],[13], [14], [1] and [2].

Of late, there has been a growing interest in preliminary analysis of MCSEM receiver data through numerical modeling. This has a motive to design optimal SBL survey variables and to obtain insights about the target responses. This work prospects has increased with many applications of the marine CSEM method. ([20], [10], [15], [17] and [11]).

This paper presents a study on the behavior of the electromagnetic waves of a curved antenna whose height (h) equals the radius (r) as a potential antenna in CSEM. In this paper we will introduce the solution of Maxwell equation one dimension for this antenna.. This antenna is located 30 m above the sea bed together with an array of stationery EM receivers for recording the EM waves (see Figure(1)). The solution of Maxwell equation will be in frequency domain. The Green Functions are used to find the solution for the poloidal and toroidal modes (that modes are unique using Helmholtz representation theorem) for the antenna. Numerical solution for the Electric field (magnitude and phase) is obtained using MATLAB software. The effect of frequency and water

* Corresponding author e-mail: dahi_80@yahoo.com

© 2016 NSP
Natural Sciences Publishing Cor.

depth on our function (Electric field) for HC detection will be observed.

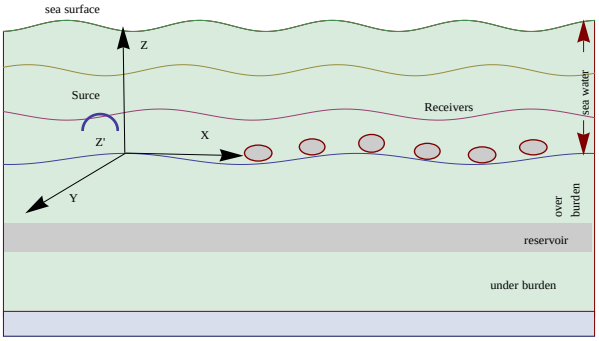

Fig. 1: A design of a basic marine CSEM (SBL) survey model. the height of antenna is $z' = 30$ meters and the height of receivers are zero and the height of water is H. the direction of upward in the direction of z .

2 GOVERNING EQUATION

Consider the diffusion of the fields of a point curved electric dipole in a one dimension layered structure. Given the Maxwell equations:

$$\begin{aligned} \nabla.E &= \frac{Q}{\varepsilon_0} \\ \nabla\times E &= -\frac{\partial B}{\partial t} \\ \nabla.B &= 0 \\ \nabla\times B &= \mu(j+\varepsilon_0\frac{\partial E}{\partial t}) \end{aligned} \tag{1}$$

where E is the electric field, B is the magnetic field, j is the current density, j_0 is the conduction current, Q is the charge density, ε_0 is the electric permittivity, μ_0 is the magnetic permeability, σ is the conductivity of medium, ω is the angular frequency and t is the time. We consider rate of change the charge is zero in our study. Furthermore from Ohms law $J^0 = \sigma E$ (displacement current) so the total current is sum of displacement current and conduction current ($J = -i\omega\varepsilon_0 E + J^0$). A low frequency (0.01 to 10 Hz), with resistivity of air and hydrocarbon of (10-11Ω) and (0.1 to 0.001 Ω) respectively are considered. Hence, the displacement current can be negligible when solving Maxwell's equation in this environment. Then the last equation of Maxwell's equation becomes.

$$\nabla\times B = \mu_0(j^0 + \varepsilon_0\frac{\partial E}{\partial t}) \tag{2}$$

We now define the coordinate system (Cartesian coordinate system), the origin point of this coordinate is on sea surface and the upward is in the positive direction of $\widehat{Z}$, and let σ be variation in the direction of $\widehat{Z}$ only. (See figure 1). The Maxwell equations will be solved in terms of poloidal and toroidal magnetic (PM and TM) modes based on a Helmholtz representation of a vector field. In horizontal planes, The PM mode is marked by electric currents, and the electric field in direction of $\widehat{Z}$ is zero. But the TM mode is associated with electric currents flowing in planes containing the vertical, and has no vertical magnetic field component.

$$V = \nabla\phi + \nabla\times(\psi\hat{z}) + \nabla\times\nabla\times(\chi\hat{z}) \tag{3}$$

By using Maxwell equation and above equation, the magnetic field can be written as:

$$B = \nabla\times(\Pi\hat{z}) + \nabla\times\nabla\times(\Psi\hat{z}) \tag{4}$$

Where the Π represented to TM mode and Ψ represented to TE mode. The source current density J^0 may be written (toroidal, consoidal and vertical parts) at the form:

$$j^0 = j_z^0\hat{z} + \nabla_h T + \nabla\times(\Upsilon\hat{z}) \tag{5}$$

Where T and Υ are the scalar functions and j_z^0 is the vertical component of current source. T and Υ are satisfy the Poisson equations:

$$\begin{aligned} \nabla_h^2 T &= \nabla_h.j_h^0 \\ \nabla_h^2\Upsilon &= -(\nabla_h\times j_h^0).\hat{z} \end{aligned} \tag{6}$$

Where ∇_h^2 is the surface Laplacian, ∇_h is the surface gradient and $\nabla_h\times$ surface curl operators.

The electric field can be written as the form:

$$E = \frac{1}{\mu\sigma}(\nabla\times\nabla\times(\Pi\hat{z})) - \frac{1}{\sigma}(j_z^0\hat{z} + \nabla_h T) - i\omega\nabla\times(\Psi\hat{z}) \tag{7}$$

$$B = \hat{z}\times\nabla_h\Pi + \nabla_h\left(\frac{\partial\Psi}{\partial z}\right) - \nabla_h^2\Psi\hat{z} \tag{8}$$

the scalar functions PM and TM mode satisfy the differential equations:

$$\nabla^2\Psi - i\omega\mu\sigma\Psi = \mu\Upsilon \tag{9}$$

$$\nabla_h^2\Pi + \sigma\frac{\partial}{\partial z}\left(\frac{\partial\Pi}{\sigma\partial z}\right) - i\omega\mu\sigma\Pi = \mu j_z^0 - \mu\sigma\frac{\partial}{\partial z}\left(\frac{T}{\sigma}\right) \tag{10}$$

From the equations 9 and 10 (diffusion waves) we can show the TM mode is driven by its vertical component and consoidal elements only whereas The PM mode is associated with the toroidal part of the source current. In addition the equations (9 and 10) are parabolic and

© 2016 NSP
Natural Sciences Publishing Cor.

hyperbolic diffusion wave equations. At horizontal interfaces The usual boundary conditions must be satisfied on the horizontal components of the electric and magnetic fields. the functions Ψ, $\frac{\partial \Psi}{\partial z}$, Π and $\frac{1}{\mu\sigma}\left(\frac{\partial \Pi}{\partial z}+\mu T\right)$ must be continues. The PM and TM modes in equations (9 and 10) are independent due to the uncoupled of boundary conditions.

3 GREEN FUNCTIONS

Since the Cartesian coordinate is used as the direction of upward in the direction of $\hat{z}$, and let the east and north be the direction of $\hat{x}$ and $\hat{y}$ respectively. The water column covers the region $-H \le z \le 0$ and the conductivity is constant with variation of vertical component $\sigma(-H)$. Let $e^{i\omega t}$ be time dependence. Since all interfaces are planar, so the horizontal Fourier will be convenient to solve the deferential equations (9 and 10) , then the Fourier transform take the form:

$$\tilde{f}(k_x,k_y)=\int_{-\infty}^{\infty} f(x,y)e^{i(k_x x+k_y y)}dxdy \tag{11}$$

$$f(x,y)=\frac{1}{(2\pi)^2}\int_{-\infty}^{\infty} \tilde{f}(k_x,k_y)e^{-i(k_x x+k_y y)}dk_x dk_y \tag{12}$$

where k_x and k_y are wavenumbers for horizontal plan. 2 has given the Green's functions solutions to the Fourier transforms of (9 and 10) for a constant conductivity ocean in the form:

$$G_\psi(z,z')=-\frac{e^{-\beta_0|z-z'|}+R_{\mathrm{L}}^{\mathrm{PM}}e^{-\beta_0(z+z'+2H)}+R_U^{\mathrm{PM}}e^{\beta_0(z+z')}+R_U^{\mathrm{PM}}R_{\mathrm{L}}^{\mathrm{PM}}e^{\beta_0(|z-z'|-2H)}}{2\beta_0\left(1-R_U^{\mathrm{PM}}R_{\mathrm{L}}^{\mathrm{PM}}e^{-2\beta_0 H}\right)} \tag{13}$$

$$G_\pi(z,z')=-\frac{e^{-\beta_0|z-z'|}+R_{\mathrm{L}}^{\mathrm{TM}}e^{-\beta_0(z+z'+2H)}+R_U^{\mathrm{TM}}e^{\beta_0(z+z')}+R_U^{\mathrm{TM}}R_{\mathrm{L}}^{\mathrm{TM}}e^{\beta_0(|z-z'|-2H)}}{2\beta_0\left(1-R_U^{\mathrm{TM}}R_{\mathrm{L}}^{\mathrm{TM}}e^{-2\beta_0 H}\right)} \tag{14}$$

Where $\beta_0^2=k^2-i\omega\mu\sigma_0$ (complex) is the ocean diffusion parameter, σ_0 is the electric conductivity of water layer, $k^2=k_x^2+k_y^2$ is the magnitude of horizontal wavenumber and R_B^A is the interaction coefficient.

Let the Earth be represented as a stack of N layers of variable with conductivity σ_i and thickness h_i terminated by a half-space that may be insulating, conducting, or a perfect conductor, Chave and Luther (1990) give the stable recursive expressions for the lower diffusion interaction coefficient in the form:

$$R_i^{\mathrm{TM}}=\frac{\chi_i+e^{-2\beta_{i+1}h_{i+1}}R_{i+1}^{\mathrm{TM}}}{1+\chi_i e^{-2\beta_{i+1}h_{i+1}}R_{i+1}^{\mathrm{TM}}} \tag{15}$$

$$R_i^{\mathrm{PM}}=\frac{\alpha_i+e^{-2\beta_{i+1}h_{i+1}}R_{i+1}^{\mathrm{PM}}}{1+\alpha_i e^{-2\beta_{i+1}h_{i+1}}R_{i+1}^{\mathrm{PM}}} \tag{16}$$

the coefficients of interface interaction are:

$$\chi_i=\frac{\beta_i\sigma_{i+1}-\beta_{i+1}\sigma_i}{\beta_i\sigma_{i+1}+\beta_{i+1}\sigma_i} \tag{17}$$

$$\alpha_i=\frac{\beta_i-\beta_{i+1}}{\beta_i+\beta_{i+1}} \tag{18}$$

The solutions of (9 and 10) within the ocean at any point for any source function, By using the Green's functions can be written in the form:

$$\tilde{\Psi}(z)=\mu\int_{-H}^{0} G_\psi(z,z')\tilde{Y}(z')dz' \tag{19}$$

$$\tilde{\Pi}(z')=\mu\int_{-H}^{0}\left(G_\pi(z,z')\tilde{j}_z^0(z')-G_\pi(z,z')\sigma\frac{\partial}{\partial z'}\left(\frac{\tilde{T}(z')}{\sigma}\right)\right)dz' \tag{20}$$

The Solutions for the EM fields are obtained using the inverse Fourier transforms (11) and calculation of the horizontal and vertical derivatives.

4 NEW ANTENNA DESIGN

Consider a curved electric dipole antenna with height (h) equals radius (r), hence in our case $R=r=h$. The centre of curved antenna is concede to the point (0 ,0 ,z') and the orientation of it in xz plane and the axes y is orthogonal to the plane as shown in Figure 2.

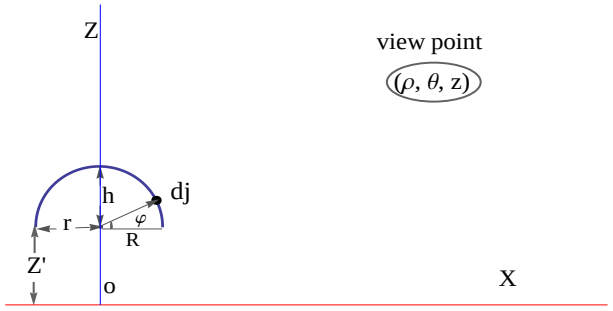

Fig. 2: Diagram showing the geometry for curved electric dipole antenna with $h=r$ and radius R . The dipole source lies in the xz plane (y Axes is orthogonal on the page) at the point $(0,0,z')$ with current flowing. the oriented of current in direction of anticlockwise. The view point point at (ρ,θ,z) is depicted by ellipse

Assume infinitesimal piece of curved antenna oriented at a anticlockwise angle φ carries the electric current density, So the infinitesimal current density can be written in the form:

$$dj^0=IR\delta(x-R\cos\varphi)\delta(y)\delta(z-z'+R\sin\varphi)d\varphi\hat{\varphi} \tag{21}$$

© 2016 NSP
Natural Sciences Publishing Cor.

where I is the electric dipole current and $\hat{\varphi}$ is the unit vector in the direction of φ that is equal to $(-\sin\varphi\hat{x} - \cos\varphi\hat{z})$, so by integral of equation (21) over semi circle $(\varphi = 0 \to \pi)$, so the source current density can be written as the form:

$$j^0(\rho,z) = -IR\delta(y)$$

$$\int_0^{\pi} \delta(x - R\cos\varphi)\delta(z - z' + R\sin\varphi)(\sin\varphi\hat{x} + \cos\varphi\hat{z})d\varphi \tag{22}$$

From equations (5,6) by taking Fourier transform of them and using equation (22) we can find:

$$\tilde{T} = -\frac{ik_x IR}{k^2}\int_0^{\pi} e^{ik_x R\cos\varphi}\delta(z - z' + R\sin\varphi)\sin\varphi d\varphi \tag{23}$$

$$\tilde{\Upsilon} = \frac{ik_y IR}{k^2}\int_0^{\pi} e^{ik_x R\cos\varphi}\delta(z - z' + R\sin\varphi)\sin\varphi d\varphi \tag{24}$$

$$\tilde{j}_z^0 = -IR\int_0^{\pi} e^{ik_x R\cos\varphi}\delta(z - z' + R\sin\varphi)\cos\varphi d\varphi \tag{25}$$

By substituting into equations (19 and 20) and taking inverse Fourier transform and using the Poisson's formula:

$$\int_0^{2\pi} e^{\pm ik\zeta\cos(\theta-\vartheta)}d\theta = 2\pi J_0(k\zeta) \tag{26}$$

where $J_0(k\zeta)$ is the first kind of Bessel function with order 0 and ϑ an arbitrary angel and $\zeta^2 = \rho^2 + R^2\cos^2\varphi - 2\rho R\cos\varphi\cos\theta$, $\rho^2 = x^2 + y^2$. We can find:

$$\Psi(\rho,z) = -\frac{\mu IR}{2\pi}\int_0^{\infty}$$

$$\int_0^{\pi} \frac{h_\psi(z,z' - R\sin\varphi)}{k}\frac{\partial J_0(k\zeta)}{\partial y}\sin\varphi d\varphi dk \tag{27}$$

and $\Pi(\rho,z) =$

$$\frac{\mu IR}{2\pi}\int_0^{\infty}\int_0^{\pi}\left(-\frac{h_\psi(z,z'-R\sin\varphi)}{k}J_0(k\zeta)\cos\varphi + \frac{\partial h_\pi(z,z'-R\sin\varphi)}{\partial z'}\frac{\partial J_0(k\zeta)}{k\partial x}\sin\varphi\right)d\varphi dk \tag{28}$$

Where $h_\psi = G_\psi - G_\psi^0$ and $\frac{\partial h_\pi}{\partial z'} = \frac{\partial G_\pi}{\partial z'} - \frac{\partial G_\pi^0}{\partial z'}$ where the superscript 0 refers to the Greens function with $k = 0$. So from equation 7 and using equations 27 and 28 we can write the electric field wave equation in Cartesian coordinate in the form:

$$E_x(\rho,z) = i\omega a$$

$$\int_0^{\infty}\left(\left(kJ_0(k\rho)\sin^2\theta + \frac{J_1(k\rho)}{\rho}\cos 2\theta\right)\frac{\partial h_\psi}{\partial z'} + \left(-kJ_0(k\rho)\cos^2\theta + \frac{J_1(k\rho)}{\rho}\cos 2\theta\right)\frac{\partial h_\pi}{\partial z}\right)dk \tag{29}$$

$$E_y(\rho,z) = i\omega a\sin\theta\cos\theta\int_0^{\infty} kJ_2(k\rho)\left(\frac{\partial h_\psi}{\partial z'} + \frac{\partial h_\pi}{\partial z}\right)dk \tag{30}$$

$$E_z(\rho,z) = i\omega a\cos\theta\int_0^{\infty} k^2 J_1(k\rho)G_\pi dk \tag{31}$$

where J_1, J_2 is the Bessel functions of first kind with the order $1,2$ respectively, and θ is the azimuth. where in our study the inline axis in the direction of x axis see figure 2.

By using equation(8) we can find the Magnetic field in cartesian coordinate in the forms:

$$B_x(\rho,z) = a\sin\theta\cos\theta\int_0^{\infty} kJ_2(k\rho)\left(\frac{\partial^2 h_\psi}{\partial z\partial z'} - h_\pi\right)dk \tag{32}$$

$$B_y(\rho,z) = a$$

$$b\int_0^{\infty}\left(-kJ_0(k\rho)\cos^2\theta + \frac{J_1(k\rho)}{\rho}\cos 2\theta\right)h_\pi dk - \int_0^{\infty}\left(kJ_0(k\rho)\sin^2\theta + \frac{J_1(k\rho)}{\rho}\cos 2\theta\right)\frac{\partial^2 h_\psi}{\partial z\partial z'}dk \tag{33}$$

$$B_z(\rho,z) = a\sin\theta\int_0^{\infty} k^2 J_1(k\rho)\left(\frac{\partial G_\psi}{\partial z'}\right)dk \tag{34}$$

5 NUMERICAL SOLUTION

Now we will give the numerical solution of electric field. The electric field equations in the directions of x and y are depending on TM and PM mode while electric field in the direction of z depends on TM only. The receivers read the data that comes from the source, interaction with sea surface and interaction with oil, and some parts where there is interaction with sea surface and oil at the same time. (Equations 12 and 13). MATLAB software is used to solve the equations (28, 29 and 30) to determine the behaviour of electromagnetic fields and Gauss-Kronrod quadrature method is used for finding the integration. These equations will be solved based on the geological model in Figure 3.

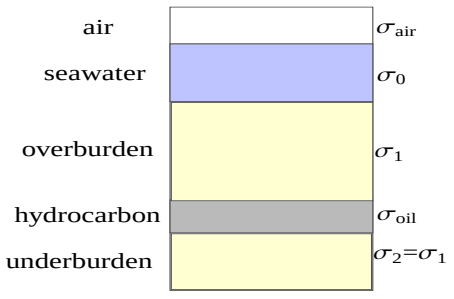

Fig. 3: sketch design for our problem

© 2016 NSP
Natural Sciences Publishing Cor.

In our solution, we let the conductivity of air be $\sigma_{air} = 10^{-11}s/m$, water $\sigma_0 = 4s/m$, overburden and underburden $\sigma_1 = \sigma_2 = 1.5s/m$ and oil $\sigma_{oil} = 0.001s/m$. the magnetic permeability are equal for all variable $(4\pi \times 10^{-7}NA^{-2})$ except for water is $0.999991 \times 4\pi \times 10^{-7}NA^{-2}$.In our model the hight of source is $30m$ and the receivers are butting on sea floor $z = 0$. the direction of x is the inline direction while the direction of broadside is any direction has an angel (azimuth) with x axis (inline) see figure (2). The curve antenna has $r = h = R = 85.9437m$ and the length of its arc equal to $270m$.

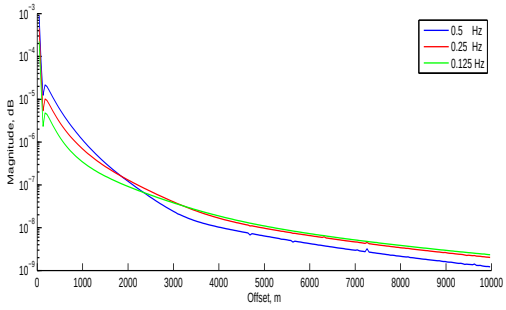

Fig. 4: magnitude of electric field (Ex) versus offset. the frequencies are 0.5, 0.25, 0.125Hz and the height of seawater is 500 m and overburden is 1000 m and the thickness of hydrocarbon layer is 100 m. with 0^o Azmuith

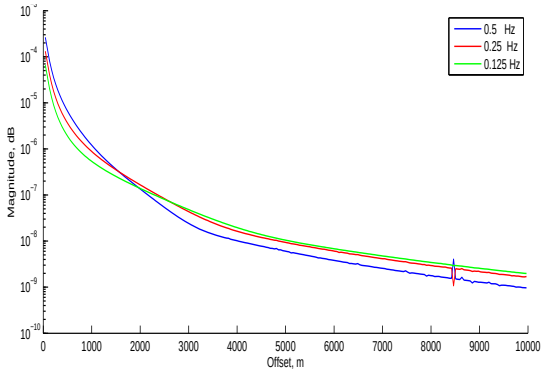

Fig. 5: magnitude of electric field (Ey) versus offset. the frequencies are 0.5, 0.25, 0.125Hz and the height of seawater is 500 m and overburden is 1000 m and the thickness of hydrocarbon layer is 100 m. with 45^o Azmuith

Figures 4- 6 shows the magnitude of the electric field with varying frequencies and azimuth. The frequencies considered in the simulations are 0.5Hz, 0.25Hz and 0.125Hz. The simulation results shows that the magnitude of electric field is high(put the approximate values of the E-field) even at offsets greater than 5km. The results also show that the highest electric field magnitude is at a frequency of 0.125Hz for all directions (x,y and z axis) which implies that the curve antenna is able to operate well even at low frequency. This result implies the potential of the new antenna in CSEM since this method makes use of low frequency.

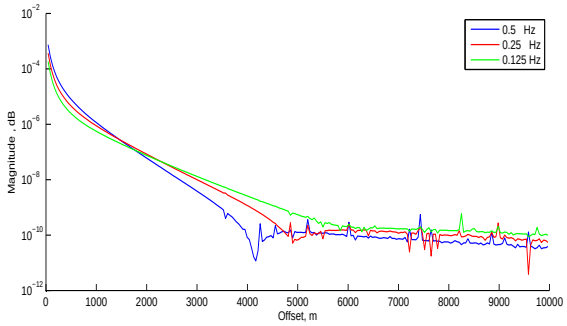

Fig. 6: magnitude of electric field (Ez) versus offset. the frequencies are 0.5, 0.25, 0.125Hz and the height of seawater is 500 m and overburden is 1000 m and the thickness of hydrocarbon layer is 100 m. with 45^o Azmuith

Simulations are also carried out to see the behavior of the E-fields when the sea water depth is varied from 200m (shallow water) to 1500m (deep water). A frequency of 0.125Hz, overburden of 1000 m and hydrocarbon thickness of 100 m are considered in the simulation. Results are shown in Figures 7, 8, 9, 10, 11 and 12.

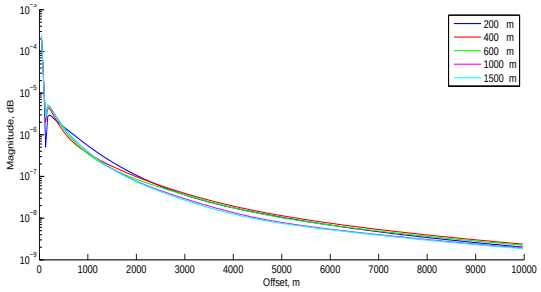

Fig. 7: . Magnitude of electric field (Ex) versus offset (using log scale for y axis). the height of seawater is 200, 400, 600, 1000, 1500 m and overburden is 1000 m and the thickness of hydrocarbon layer is 100 m. and the frequency is 0.125H. with 0^o Azmuith

The Electric field values along Ex component is higher at the near offset and are large for shallow water

© 2016 NSP
Natural Sciences Publishing Cor.

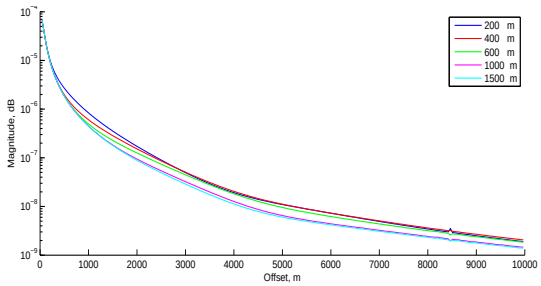

Fig. 8: . Magnitude of electric field (Ey) versus offset (using log scale for y axis). the height of seawater is 200, 400, 600, 1000, 1500 m and overburden is 1000 m and the thickness of hydrocarbon layer is 100 m. and the frequency is 0.125H. with 45^o Azmuith

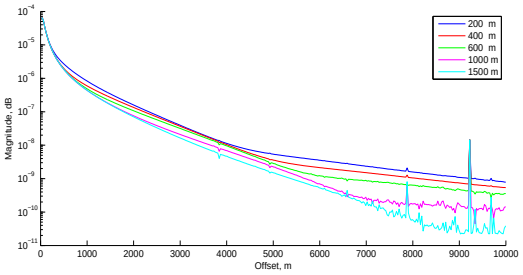

Fig. 11: . Magnitude of electric field (Ey) versus offset (using log scale for y axis). the height of seawater is 200, 400, 600, 1000, 1500 m and overburden is 1000 m, without hydrocarbon layer and the frequency is 0.125H. with 45^o Azmuith

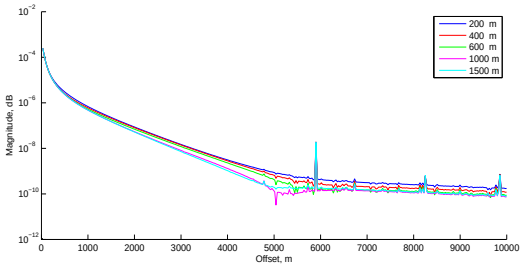

Fig. 9: . Magnitude of electric field (Ez) versus offset (using log scale for y axis). the height of seawater is 200, 400, 600, 1000, 1500 m and overburden is 1000 m and the thickness of hydrocarbon layer is 100 m. and the frequency is 0.125H. with 0^o Azmuith

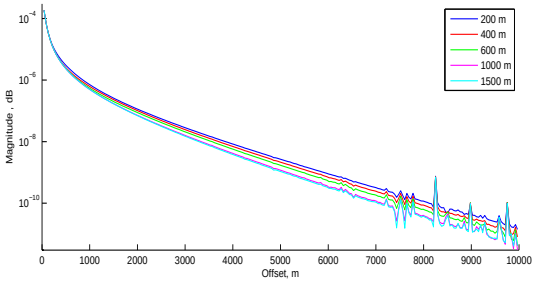

Fig. 12: Magnitude of electric field (Ez) versus offset (using log scale for y axis). the height of seawater is 200, 400, 600, 1000, 1500 m and overburden is 1000 m. without hydrocarbon layer. and the frequency is 0.125H. with 0^o Azmuith

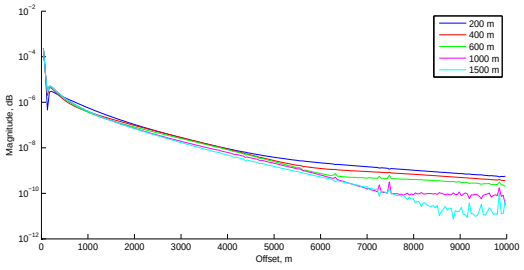

Fig. 10: . Magnitude of electric field (Ex) versus offset (using log scale for y axis). the height of seawater is 200, 400, 600, 1000, 1500 m and overburden is 1000 m,without hydrocarbon layer and the frequency is 0.125H. with 0^o Azmuith

environment Also, the E-field along the Ey component decreases as the offset increases. As Ez is the vertical component, the magnitude of Ez is small for deep water but big for shallow water environment.

Now we give the behavior of electric field for variation of overburden. The frequency is 0.125Hz, the height of sea water is 500m and the thickness of hydrocarbon is 100 m.

From the Figures 13, 14 and 15 it is clear that the magnitude of electric field is big for shallow overburden and vice versa. The reason is that, the electric field wave will decay faster when the thickness of the overburden increases. These results have shown that the new antenna is able to detect the different resistive layers just like the current horizontal antenna.

© 2016 NSP
Natural Sciences Publishing Cor.

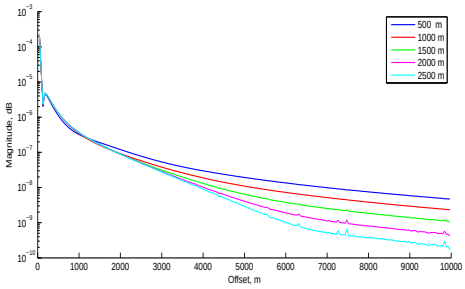

Fig. 13: Magnitude of electric field (Ex) versus offset (using log scale for y axis). the height of seawater is 500 m and overburdens are 500, 1000, 1500, 2000, 2500 m and the thickness of hydrocarbon layer is 100 m. and the frequency is 0.125H. with 0^o Azmuith

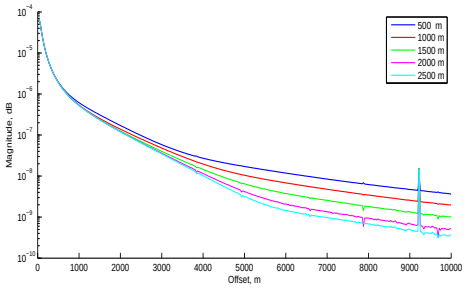

Fig. 14: Magnitude of electric field (Ey) versus offset (using log scale for y axis). the height of seawater is 500 m and overburdens are 500, 1000, 1500, 2000, 2500 m and the frequency is 0.125H. with 45^o Azmuith

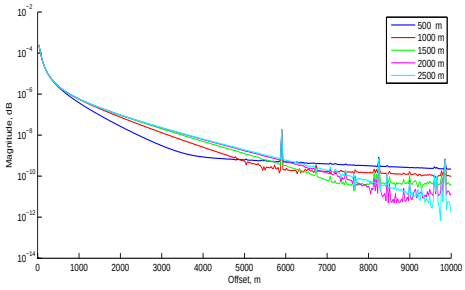

Fig. 15: Magnitude of electric field (Ez) versus offset (using log scale for y axis). the height of seawater is 500 m and overburdens are 500, 1000, 1500, 2000, 2500 m and and the frequency is 0.125H. with 0^o Azmuith

6 CONCLUSION

This paper introduces the solution of Maxwell Equation in one dimension using a new design of antenna with $h = r$. It has been shown the new antenna is able to detect the resistivity contrast in homogenous layers media. It is observed that smaller frequencies are better in detecting the resistive layers. Difference in the Electric field is also observed in the presence of hydrocarbon. These simulations seem to indicate that this antenna has the potential to be used as a source of EM waves.

Acknowledgement

The authors would like to acknowledge the university for the financial assistance granted to carry out this study.

References

[1] Chave, A. D., and C. S. Cox, (1982), Controlled electromagnetic sources for measuring electrical conductivity beneath the oceans: Journal of Geophysical Research, 87, 5327-5338.

[2] Chave, A.D. and Luther, D.S., 1990. Low frequency, motionally induced electromagnetic fields in the ocean, 1 , Theor y, J. geophys. R es., 95, 71857200.

[3] Coggon, J. H., and H. F. Morrison, (1970), Electromagnetic investigation of the sea floor: Geophysics, 35, 476 - 489, doi: 10.1190/1.1440109.

[4] Constable, S., A. Orange, G. M. Hoversten, and H. F. Morrison, (1998), Marine magnetotellurics for petroleum exploration: Part 1 - A sea-floor equip-ment system: Geophysics, 63, 816 - 825, doi: 10.1190/1.1444393.

[5] Constable, S., Srnka, L.J (2007) : An introduction to marine controlled-source electromagnetic methods for hydrocarbon exploration Geophysics 72, WA3.

[6] Cox, C. S., J. H. Filloux, and J. C. Larsen, (1971), Electromagnetic studies of ocean currents and electrical conductivity below the ocean floor, in A. E. Maxwell, ed., The sea, Vol. 4, Part I: Wiley Inter science, 637-693.

[7] Demuth, H., Beale, M., Hagan, M.: Neural Network Toolbox Users Guide 19922008 by The MathWorks, Inc.,3 Apple Hill Drive, Natick, MA: 01760-2098 (2008).

[8] Edwards, R. N., L. K. Law, P. A. Wolfgram, D. C. Nobes, M. N. Bone, D. F.Trigg, and J. M. DeLaurier, (1985), First results of the MOSES experiment: Sea sediment conductivity and thickness determination, Bute Inlet, British Columbia, by magnetometric offshore electrical sounding: Geophysics, 50 , 153-161, doi: 10.1190/1.1441825.

[9] Eidesmo. T, S. Ellingsrud, L.M. MacGregor, S. Constable, M.C. Sinha, S. Johansen, F.N. Kong and H. Westerdahl, (2002), Sea Bed Logging (SBL), A new method for remote and direct identification of hydrocarbon filled layers in deepwater areas, First Break, 20(3), 144-52 .

[10] Frenkel, M.A. and Davydycheva, S., 2012, To CSEM or not to CSEM? Feasibility of 3D marine CSEM for detecting small targets. The Leading Edge, 31, 435446. doi: 10.1190/tle31040435.1.

[11] Hangilro Jang, Hannuree Jang, Hee Joon Kim. (2015) Three-dimensional electromagnetic responses of disk-shaped hydrocarbon reservoir in marine sediments. Geosciences Journal 19:2, 305.

[12] Hesthammer, J., Boulaenko, M. (2007): The potential of CSEM technology, Geo-Expro, 4, 2007, pp. 52-58, and HGS Bulletin, pp. 23-43 December, Rocksource ASA.

© 2016 NSP
Natural Sciences Publishing Cor.

[13] Hoversten, G. H., S. Constable, and H. F. Morrison, (2000), Marine magnetel-lurics for base salt mapping: Gulf of Mexico fieldtest at the Gemini struc-ture: Geophysics, 65, 1476 -1488, doi: 10.1190/1.1444836.
[14] Hoversten, G. M., H. F. Morrison, and S. Constable, (1998), Marine magnetotellurics for petroleum exploration: Part 2 - Numerical analysis of subsalt resolution: Geophysics, 63, 826 - 840, doi: 10.1190/1.1444394.
[15] Key, K., 2012, Marine electromagnetic studies of seafloor resources and tectonics. Surveys in geophysics, 33, 135167. doi :10.1007/s10712-011-9139-x
[16] Lϕseth. L.O., H.M. Pedersen , T. Schaug-Pettersen , S. Ellingsrud , T. Eidesmo, (2008), A scaled experiment for the verification of the SeaBed Logging method, Journal of Applied Geophysics 64 47 - 55.
[17] Strack, K.M., 2014, Future directions of electromagnetic methods for hydrocarbon applications. Surveys in Geophysics, 35, 157177.doi: 10.1007/s10712-013-9237-z.
[18] Wolfgram, P. A., R. N. Edwards, L. K. Law, and M. N. Bone, (1986), Polymetallic sulfide exploration on the deep sea floor: The feasibility of the MINI-MOSES experiment: Geophysics, 51, 1808 -1818, doi: 10.1190/1.1442227.
[19] Young, P. D., and C. S. Cox, (1981), Electromagnetic active source sounding near the East Pacific Rise: Geophysical Research Letters, 8 , 1 043-1046.
[20] Zhdanov, M.S., 2010, Electromagnetic geophysics: Notes from the past and the road ahead. Geophysics, 75, 74A4975A66. doi: 10.1190/1.3483901.

Elsayed Dahy was born in Egypt. His obtained Bachelor's Degree in Mathematics from University of Al-Azhar in 2003 and Master's Degree (M.Sc. Differential Geometry) from Assuit University, Egypt in 2011. He started his academic career as an academic staff of the department of Mathematics, Faculty of Science, University of Al-Azhar since 2006. He has also published in both local and International scientific journals and conference articles. Presently he belongs to the Novel EM Transmitter in Conducting Medium research group Universiti Teknologi PETRONAS in Malaysia as a Doctoral research fellow/research officer.

Afza Shafie is currently a Senior Lecturer with the Fundamental and Applied Science Department (FASD) at Univerisiti Teknologi PETRONAS. She holds a Bachelor and a Master degree in mathematics and statistics respectively. In addition she has a PhD in Systems Technology. Her interest is in mathematical and statistical modeling. Her research includes the application of electromagmetics in hydrocarbon detection in Malaysian waters, application of electromagnetic and nanofluids in enhanced oil recovery, data analysis for offshore structures. Some of her research has been funded by Petroleum Research Fund (PRF), Yayasan ? UTP grant, the Prototype Research Grant (PRGS) and the Fundamental Research Grant (FRGS) from the Ministry of Education Malaysia. She is also involved in a joint project with the Ipoh Kiwanis Down Syndrome Centre and Research Center of Raja Permaisuri Bainun General Hospital in Ipoh. She is a member of European Association of Geoscientists and Engineers (EAGE), Persatuan Matematik Malaysia (PESAMA) and the International Society of Nanoscience. Her work has been presented in international conferences and published in ISI journals.

Noorhand Yahya is a Professor of Physics at UTP Malaysia. She obtained her B.Sc. (Hons), M.Sc. and PhD degrees in physics from Universiti Pertanian and Putra Malaysia in 1996, 1998 and 2001 respectively. Since April 2011 she has been holding the Dean position of the Faculty of Sciences and Information Technology. She has published more than 120 journal papers, 10 patents including one for commercialization called NCZ method on ONE-STEP urea synthesis in a high density magnetic flux with new catalyst support. Since 2002 she has been awarded 24 international, local invention research awards including Best Russian Award 2010 and Gold Medal from Innova-Eureka, and participation in more than 50 scientific conferences locally and worldwide. She also spearheaded research on Electromagnetics at UTP and was awarded with PRF to develop an EM Transmitter for Shallow Water Environment.

© 2016 NSP
Natural Sciences Publishing Cor.